

T Cell Receptor–MHC Class I Peptide Interactions: Affinity, Kinetics, and Specificity

Maripat Corr,* Alfred E. Slanetz, Lisa F. Boyd, Marie T. Jelonek, Sergei Khilko, Basel K. Al-Ramadi, Young Sang Kim,† Stephen E. Maher, Alfred L. M. Bothwell, David H. Margulies‡

The critical discriminatory event in the activation of T lymphocytes bearing $\alpha\beta$ T cell receptors (TCRs) is their interaction with a molecular complex consisting of a peptide bound to a major histocompatibility complex (MHC)–encoded class I or class II molecule on the surface of an antigen-presenting cell. The kinetics of binding were measured of a purified TCR to molecular complexes of a purified soluble analog of the murine MHC class I molecule H-2L^d (sH-2L^d) and a synthetic octamer peptide p2CL in a direct, real-time assay based on surface plasmon resonance. The kinetic dissociation rate of the MHC-peptide complex from the TCR was rapid (2.6×10^{-2} second⁻¹, corresponding to a half-time for dissociation of approximately 27 seconds), and the kinetic association rate was 2.1×10^5 M⁻¹ second⁻¹. The equilibrium constant for dissociation was approximately 10^{-7} M. These values indicate that TCRs must interact with a multivalent array of MHC-peptide complexes to trigger T cell signaling.

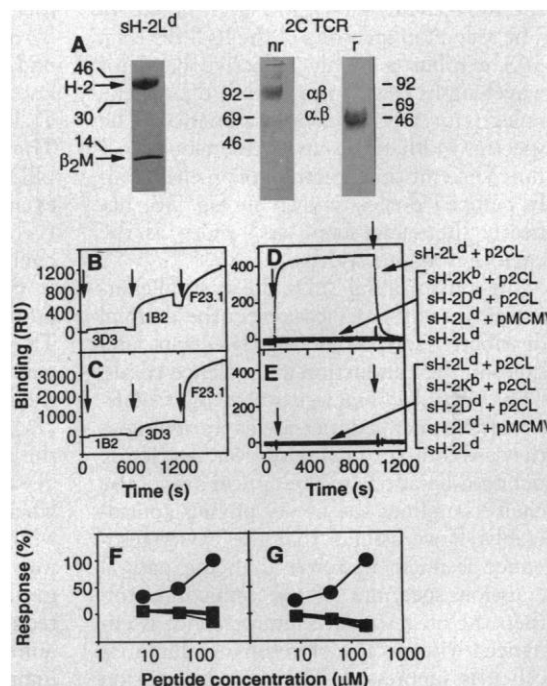
Considerable interest and experimentation have been devoted to the quantitative study of the interaction of TCRs with MHC-peptide complexes, including studies of purified MHC molecules (1–3) or TCRs (4). We used engineered analogs of TCR and MHC class I molecules and synthetic peptides to examine peptide-dependent binding of MHC to TCRs using only purified components with surface plasmon resonance (SPR). SPR detection allows the quantitative real-time measurement of binding interactions between immobilized and solution-phase ligands without radiolabeling or biochemical tagging (5). We used an sH-2L^d class I molecule (secreted in biologically active form by L cell transfectants) that was purified by immunoabsorbent chromatography (Fig. 1A). To study the interaction of an $\alpha\beta$ TCR with an MHC-peptide complex, we used two TCRs engineered for cell surface expression by means of a phosphatidylinositol linkage in a transfected T cell thymoma (6) (Fig. 1A). One of these TCRs, 2C, derived from a cytolytic T cell clone originally identified for its alloreactivity against H-2L^d, is specific for H-2L^d complexed to a self peptide, p2CL (LSPFFFDL) (7, 8). The purified

TCRs were covalently linked to the dextran-modified gold surface of an SPR biosensor chip and retained reactivity with both receptor-specific (anti-clonotypic) monoclonal antibodies (mAbs) and variable region (V_β)–specific and constant region (C_β)–specific mAbs. The immobilized 2C $\alpha\beta$ TCR showed little binding to the control mAb 3D3 (9) but sequentially

bound to the clonotype mAb 1B2 (10) and to the V_β8-specific mAb F23.1 (11) (Fig. 1B), confirming that these mAbs bind to distinct sites on the TCR. Similarly, the immobilized D10 TCR specifically bound to both the 3D3 clonotype mAb and the V_β8-specific F23.1 and did not bind to the 1B2 mAb (Fig. 1C).

Purified MHC molecules exposed to various peptides were passed over the TCR-coupled biosensor surfaces (Fig. 1, D and E). A binding signal above the background was consistently observed only when the 2C TCR was exposed to a mixture of sH-2L^d and the p2CL peptide (Fig. 1D). No other MHC molecule tested, either with or without p2CL or with other peptides, revealed any binding to the solid-phase 2C TCR. The control surface prepared with the D10 TCR failed to bind any of these MHC-peptide combinations (Fig. 1E). Eight other viral and self peptides that bind well to sH-2L^d (12) failed to generate sH-2L^d–peptide complexes that could detectably bind the 2C TCR (Fig. 1, F and G). Exposure of sH-2L^d to several other peptides, including APAAAAAAL (8, 12), failed to generate complexes that bound to the receptor (13). Although 2C TCR transgenic animals expressing H-2K^b exhibited positive selection and increased the number of cells expressing this TCR (14), we could not detect binding of sH-2K^b (a preparation known to be largely complexed to self peptides, but

Fig. 1. Expression and binding specificity of chimeric purified TCRs (31–33). (A) SDS-PAGE analysis of purified sH-2L^d (MHC) and of purified 2C TCR (TCR). The sH-2L^d was examined on a 20% polyacrylamide gel and stained with Coomassie blue; TCR was examined with (r) and without (nr) prior reduction in SDS-PAGE (12.5% gel was silver-stained). Molecular size markers are in kilodaltons; β_2 M, β_2 -microglobulin. Kinetic binding curves (sensorgrams) of antibodies binding to 2C TCR (B) or D10 TCR (C) are also shown, as are sensorgrams of the indicated MHC-peptide complexes binding to biosensor surfaces coupled with 2C TCR (D) or with D10 TCR (E). All binding curves are expressed as resonance units (RU) as a function of time. (F) The equilibrium binding value at the indicated peptide concentrations of sH-2L^d complexed with p2CL (LSPFFFDL) (filled circles) or with each of the following peptides: pMCMV (YPHFMPTNL); p23 (APLEANYQAF); p30 (APQKAGG-FLM); or p29 (YPNVNIHNF) (all as filled squares). (G) Data as in (F) for p2CL (filled circles) and p27 (APQPPLYQL); p25B (APQRGRENF); pLCMV (RPQASGVYM); (APQPGMENF) (filled squares) (β). The arrows in (B), (C), (D), and (E) show the injection of the indicated analytes. The first arrow in (D) and (E) indicates the initiation of the injection of the MHC-peptide complexes; the second indicates the beginning of the buffer washout. All measurements were made at 25°C.



M. Corr, L. F. Boyd, M. T. Jelonek, S. Khilko, D. H. Margulies, Molecular Biology Section, Laboratory of Immunology, National Institute of Allergy and Infectious Diseases, NIH, Bethesda, MD 20892, USA.

A. E. Slanetz, B. K. Al-Ramadi, Y. S. Kim, S. E. Maher, A. L. M. Bothwell, Section of Immunobiology and Department of Biology, Yale Medical School, New Haven, CT 06520, USA.

*Present address: Department of Medicine, University of California at San Diego, San Diego, CA 92093, USA.

†Present address: Department of Biochemistry, College of Natural Sciences, Chungnam National University, Daejeon, Republic of Korea.

‡To whom correspondence should be addressed.

with a proportion of active peptide binding sites) or of sH-2K^b-p2CL complexes to the 2C TCR. Thus, either the affinity of the H-2K^b-peptide complex for the TCR was beyond the limit of detection in our assay system or positive selection of the 2C TCR mediated by H-2K^b requires a peptide other than p2CL in transgenic mice.

Once the peptide and MHC specificity of the binding to the immobilized TCR were established, we evaluated the dose dependence of the binding (Fig. 2). Binding curves of the interaction of sH-2L^d-p2CL complexes with the TCR, at constant sH-2L^d concentration (10 μg/ml, 0.17 μM) and titrated concentrations of the peptides revealed that the dose was dependent on peptide concentration with a half-maximal binding at a peptide concentration of 0.51 ± 0.064 μM (Fig. 2, A and B); this indicates that half of the active sH-2L^d molecules formed a complex with p2CL at a concentration consistent with the independently measured affinity of the binding of p2CL with sH-2L^d (15). In the presence of an excess of p2CL (250 μM), binding was

dependent on the concentration of sH-2L^d, with half-maximal binding at a concentration of sH-2L^d of 0.047 ± 0.0053 μM (Fig. 2, C and D). The proportion of available peptide binding sites in this sH-2L^d preparation was determined to be 40% (16). Under conditions of peptide excess, all available peptide binding sites on sH-2L^d were occupied; therefore, the half-maximal value serves to indicate the dissociation constant for the interaction of the MHC-peptide complexes with the immobilized TCR. The specificity of the interaction between the solid-phase purified 2C TCR and the preformed sH-2L^d-p2CL complexes was confirmed by addition of the purified TCR in solution, which blocked the binding of the MHC-peptide complexes (Fig. 2E). To evaluate the possibility that free peptide might affect the binding of MHC-peptide complexes to the solid-phase TCR, we formed sH-2L^d-p2CL complexes and then isolated them free of excess peptide. Such repurified complexes gave identical binding curves (17).

Kinetic parameters that govern the in-

teraction of the MHC-peptide complexes with the TCR were evaluated. The data for the association phase were fit to a single exponential expression descriptive of a classical two-component binding reaction (Fig. 3A). These fits were acceptable, but the residuals (that is, the differences between the experimental data and the calculated curves) suggested that the single exponential description of the association phase was not complete. A double exponential expression, describing two simultaneous binding reactions (18), was also fit to the association phase data (Fig. 3C), and the plotted residuals indicated that these curves fit the data more closely. The association phase data of the rapid component were evaluated for the concentration dependence of the apparent constant and provided an association rate constant, k_{on} , of $2.1 \times 10^5 \text{ M}^{-1} \text{ s}^{-1}$ (Table 1). We also analyzed the dissociation phase data by curve fitting to both single and double first-order exponential expressions (Fig. 3, B and D, and Table 1). The data fit well to a single exponential expression with minimal improvement by the addition of a second term. The measured dissociation rate constant (k_{off}) was $2.6 \times 10^{-2} \text{ s}^{-1}$, a value corresponding to a half-time ($t_{1/2}$) of approximately 27 s.

This analysis permitted evaluation of the binding of MHC-peptide complexes to a cognate peptide-dependent, allospecific TCR by both equilibrium and kinetic measures. Equilibrium values lead to a dissociation constant (K_d) value of $4.7 \times 10^{-8} \text{ M}$ (Fig. 2). Kinetic analysis (Fig. 3 and Table 1) revealed a moderate to rapid association rate ($2.1 \times 10^5 \text{ M}^{-1} \text{ s}^{-1}$) and very rapid dissociation rate ($2.6 \times 10^{-2} \text{ s}^{-1}$), leading to a calculated value of K_d (k_{off}/k_{on}) of $1.2 \times 10^{-7} \text{ M}$, which is internally consistent with the values obtained from the equilibrium data. The value for k_{on} approaches that observed for interactions between protein antigens and antibodies [$\sim 10^6$ to $10^7 \text{ M}^{-1} \text{ s}^{-1}$ (15)] and is considerably faster than those values observed for interactions between peptides and MHC molecules [$\sim 10^0$ to $10^4 \text{ M}^{-1} \text{ s}^{-1}$ (19–21)]. The rapid dissociation of the sH-2L^d-p2CL peptide complex from the 2C TCR contrasts with the slow dissociation rates of peptides from either class I or class II MHC molecules [characterized by $t_{1/2} = 1$ to >100 hours (22, 23)] and is faster than the dissociation of antibody-protein-antigen interactions of moderate affinity [$t_{1/2} =$ minutes to hours (19)].

Soluble H-2K^b inhibits the apparently low-affinity interaction of cells expressing the H-2K^b mutation H-2K^{bm10} with an H-2K^b-restricted allospecific T cell hybridoma (2). The affinity of the H-2K^b-TCR interaction is approximately 10^{-5} M and may be considered to be as high as $\sim 10^{-7} \text{ M}$ on the assumption that 1% of the H-2K^b

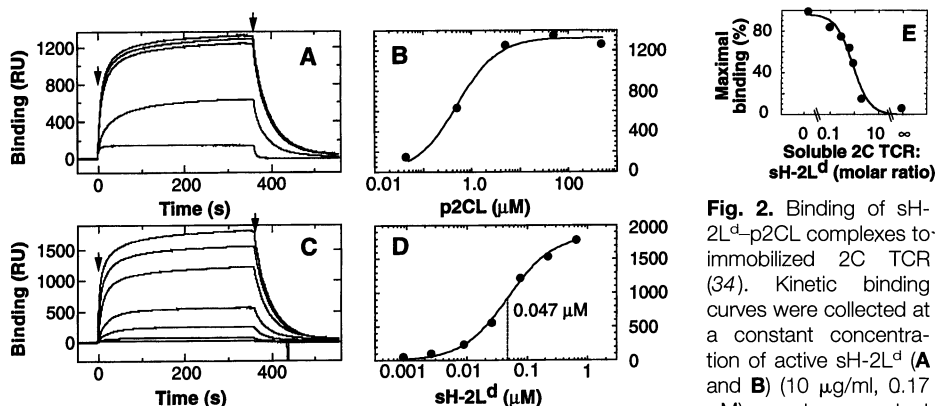


Fig. 2. Binding of sH-2L^d-p2CL complexes to immobilized 2C TCR (34). Kinetic binding curves were collected at a constant concentration of active sH-2L^d (A and B) (10 μg/ml, 0.17 μM) or at a constant

concentration of p2CL (250 μM) (C and D), and the equilibrium values for binding were plotted as a function of concentration (B and D). (E) Competition of binding of sH-2L^d with soluble 2C TCR. The first arrow in (A) and (C) indicates the initiation of the injection of the solution-phase ligand; the second indicates the beginning of the buffer washout.

Fig. 3. Curve fitting of association (A and C) and dissociation (B and D) phases of binding curves to single (A and B) and double (C and D) exponential expressions (35).

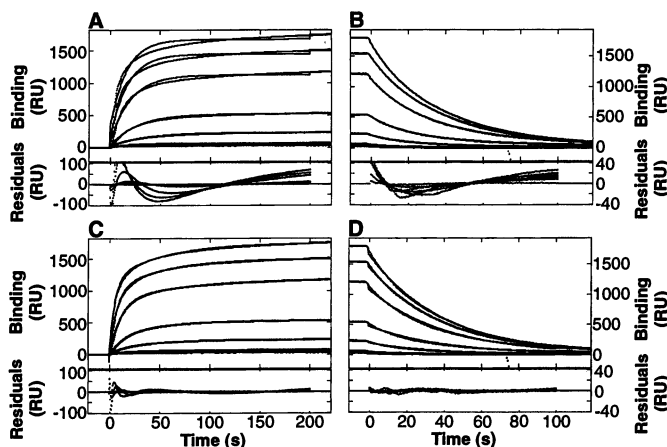


Table 1. Kinetic association and dissociation rates of the sH-2L^d-p2CL interaction with immobilized 2C TCR. Data points for the association and dissociation phases of the four binding experiments done at the higher concentrations of Fig. 3 were analyzed by curve fitting to both single (k_{obs} , k_{on} , and k_{off}) and double ($k_{\text{obs,fast}}$, $k_{\text{on,fast}}$, and $k_{\text{off,slow}}$) exponential expressions as suggested (18). Association and dissociation phase data for the 401 data points of the first 200 s were fit with the single or double exponential equations as described (35). For k_{obs} and $k_{\text{obs,fast}}$ (the observed rate constants), the values were plotted as a function of concentration [taking into account the 40% fraction of active molecules (16) (Fig. 3)], and the slope of the least squares linear fit of this curve was determined. For the double exponential association rate curve fitting, the fast component accounted for 62, 72, 65, and 68% of the molecules for the concentrations 0.02, 0.072, 0.23, and 0.67 μM , respectively. Mean values for k_{off} and $k_{\text{off,slow}}$ were 0.026 ± 0.00050 and $0.020 \pm 0.0046 \text{ s}^{-1}$, respectively. Values for k_{on} were determined by curve fitting to the linear regression of the k_{obs} dependence on concentration.

Concentration (μM)	Association phase		Dissociation phase	
	k_{obs} (s^{-1})	$k_{\text{obs,fast}}$ (s^{-1})	k_{off}^* (s^{-1})	$k_{\text{off,slow}}^*$ (s^{-1})
0.67	0.059 ± 0.002	0.21 ± 0.003	0.026	0.024
0.23	0.055 ± 0.001	0.16 ± 0.002	0.025	0.024
0.072	0.049 ± 0.001	0.095 ± 0.001	0.025	0.017
0.02	0.037 ± 0.0003	0.065 ± 0.004	0.026	0.015
	$k_{\text{on}} = 2.6 \times 10^4 \text{ M}^{-1} \text{ s}^{-1}$		$k_{\text{on,fast}} = 2.1 \times 10^6 \text{ M}^{-1} \text{ s}^{-1}$	

*For all values, SD < 1.6%.

molecules contain appropriate self peptide. Recognition by an allospecific cytotoxic T lymphocyte is blocked by nanomolar concentrations of a soluble H-2K^b-immunoglobulin (Ig) chimera, but divalency obviates accurate estimation of the affinity of the MHC-TCR interaction (3). Purified I-E^k-pigeon cytochrome c peptide complexes have been used to compete for the binding of monovalent ¹²⁵I-labeled fragments (Fab) of V_β-specific mAb to an antigen-specific, MHC-restricted hybridoma (1). The mAb was assumed to be a complete antagonist for the MHC-peptide binding site, and the affinity of this TCR for the MHC-peptide complex was estimated as 4×10^{-5} to 6×10^{-5} M. A monovalent chimeric molecule (TCR-Igκ) has been used to block the functional presentation of I-E^d-dependent, antigen-specific hybridomas and revealed an affinity of between 10^{-5} and 5×10^{-6} M (4). Because these studies used cell-surface TCRs or MHC as one component of the binding reaction, they did not formally eliminate contributions of accessory molecules from the measured parameters.

Our measurements indicate that the interaction of the MHC-peptide complex with the TCR is a binding reaction more like an antibody-antigen reaction than like a peptide-MHC one, presumably because this is a surface-to-surface interaction in which the MHC-bound peptide, folded as an intrinsic component of the MHC, binds the TCR as a unit. In the absence of additional contributions by accessory molecules, the interaction of the 2C TCR with the sH-2L^d-p2CL complex is one not only of moderate affinity, but of moderate association rate and rapid off rate. Such a rapid off rate ($t_{1/2} = \sim 27$ s) suggests that a single interaction of a TCR and an MHC-peptide complex would have insufficient residence

time to trigger a TCR-mediated signal. A decreased effective off rate (a longer $t_{1/2}$) could be achieved by multivalent binding within a small surface area at the interface between the T cell and the antigen-presenting cell and could establish a threshold requiring two or more complexes, depending on the particular kinetic characteristics of the MHC-TCR interaction. Such multivalent binding might provide the nucleus for the recruitment of additional interactions of accessory molecules, as suggested by experiments evaluating the avidity of LFA-1-ICAM-1 (leukocyte function-associated molecule-intercellular adhesion molecule) interactions in resting as compared to activated cells (24, 25). Our model places the TCR-MHC peptide interaction, rather than that of accessory molecules, as the critical initial step. This contrasts with another low-affinity model in which the initial interaction is a result of accessory molecules (1). The biphasic character of the binding curves of our real-time kinetics measurements also suggests that the binding of MHC-peptide complexes with immobilized TCRs is not a simple interaction but may require structural readjustment or conformational changes of the components.

Note added in proof: After this manuscript was submitted for publication, the interaction of H-2L^d-p2CL complexes with 2C-expressing cytotoxic T lymphocytes was reported (36).

REFERENCES AND NOTES

1. K. Matsui *et al.*, *Science* **254**, 1788 (1991).
2. J. Schneck *et al.*, *Cell* **56**, 47 (1989).
3. J. Dalporto *et al.*, *Proc. Natl. Acad. Sci. U.S.A.* **90**, 6671 (1993).
4. S. Weber *et al.*, *Nature* **356**, 793 (1992).
5. U. Jönsson *et al.*, *Biotechniques* **11**, 620 (1991).
6. A. Slanetz and A. Bothwell, *Eur. J. Immunol.* **21**, 179 (1991).

7. K. Udaka *et al.*, *Cell* **69**, 989 (1992).
8. Abbreviations for the amino acid residues are A, Ala; C, Cys; D, Asp; E, Glu; F, Phe; G, Gly; H, His; I, Ile; K, Lys; L, Leu; M, Met; N, Asn; P, Pro; Q, Gln; R, Arg; S, Ser; T, Thr; V, Val; W, Trp; and Y, Tyr.
9. J. Kaye, S. Porcellini, J. Tite, B. Jones, J. Janeway, *J. Exp. Med.* **158**, 836 (1983).
10. D. Kranz *et al.*, *Proc. Natl. Acad. Sci. U.S.A.* **81**, 573 (1984).
11. U. D. Staerz, H.-G. Rammensee, J. D. Benedetto, M. J. Bevan, *J. Immunol.* **134**, 3994 (1985).
12. M. Corr *et al.*, *J. Exp. Med.* **176**, 1681 (1992).
13. M. Corr *et al.*, unpublished observations.
14. W. Sha *et al.*, *Proc. Natl. Acad. Sci. U.S.A.* **87**, 6186 (1990).
15. M. T. Jelonek and D. H. Margulies, unpublished observations.
16. Values for the concentration of preparations of sH-2L^d are based on the protein concentration corrected for the proportion of molecules capable of binding peptide, which was estimated to be 40% in an assay of peptide-dependent epitope induction (12). This assay uses immobilized mAb 30-5-7S (which recognizes a peptide-dependent epitope of the $\alpha 2$ domain of H-2L^d) for SPR measurement of the amount of peptide-inducible H-2L^d binding activity. Thus, base line (peptide-independent) and peptide-dependent (at saturating amounts of peptide) values for 30-5-7S binding were determined. The proportion of peptide-dependent binding to the mAb is considered to be the proportion of available peptide binding sites. Over a period of several years, purified sH-2L^d preparations exhibited from 15 to 70% available sites, as estimated from such assays. In a previous study of the equilibrium binding of radiolabeled synthetic peptide to purified sH-2L^d, high-affinity peptide binding sites accounted for 12% of the available protein [L. F. Boyd, S. Kozlowski, D. H. Margulies, *Proc. Natl. Acad. Sci. U.S.A.* **89**, 2242 (1992)].
17. L. F. Boyd and D. H. Margulies, unpublished observations.
18. D. J. O'Shannessy *et al.*, *Anal. Biochem.* **212**, 457 (1993).
19. J. A. Berzofsky, S. L. Epstein, I. Berkower, in *Fundamental Immunology*, W. Paul, Ed. (Raven, New York, 1993), pp. 421-465.
20. J. Rothbard and M. Geffer, *Annu. Rev. Immunol.* **9**, 527 (1991).
21. S. Khilko, M. T. Jelonek, L. F. Boyd, D. H. Margulies, unpublished observations.
22. D. H. Margulies, M. Corr, L. F. Boyd, S. N. Khilko, *J. Mol. Recognit.* **6**, 59 (1993).
23. S. Buus *et al.*, *Cell* **47**, 1071 (1986).
24. M. L. Dustin and T. A. Springer, *Nature* **341**, 619 (1989).
25. T. A. Springer, *ibid.* **346**, 425 (1990).
26. Y. Takebe *et al.*, *Mol. Cell. Biol.* **8**, 466 (1988).
27. S. C. Hong *et al.*, *Cell* **69**, 999 (1992).
28. D. Kranz, S. Tonegawa, H. Eisen, *Proc. Natl. Acad. Sci. U.S.A.* **81**, 7922 (1984).
29. R. T. Kubo, W. Born, J. W. Kappler, P. Marrack, M. Pigeon, *J. Immunol.* **142**, 2736 (1989).
30. M. Corr, L. F. Boyd, E. A. Padlan, D. H. Margulies, *J. Exp. Med.* **178**, 1877 (1993).
31. Soluble MHC class I molecules were purified (11) and analyzed by SDS-polyacrylamide gel electrophoresis (SDS-PAGE). Chimeric genes encoding the V_αC_α and V_βC_β portions of the cloned TCR complementary DNAs (cDNAs) from the 2C cytolytic T cell clone (10) were engineered in a modification of the pFRSV plasmid (6). We modified the SV40 early promoter of pFRSV by replacing the 600-bp Kpn I-Eco RI fragment with a ~700-bp Sal I-Eco RI fragment (after rendering the Kpn I and Sal I ends blunt with Klenow polymerase) containing the SR α promoter derived from pCDL1 (26), resulting in pFRSV-SR α . The unique Eco RI site was then used for cloning the filled-in TCR α -Thy-1 and TCR β -Thy-1 fragments of the previously described pFRSV (TCR α -Thy-1) and pFRSV (TCR β -Thy-1) recombinants (6) by blunt end ligation. To generate the D10 glycosyl-phosphatidylinositol (GPI)-TCR, we replaced the V_α of the 2C-derived clone with the V_α of D10 (27) using the Eco RI-Hind III fragment containing V_α plus ~200 bp of the C_α region. Similarly, the V_β of the 2C clone was replaced by the V_β of the D10 cDNA (27) using an

- each RI-Nco I fragment. The 2C GPI-TCR α and β and the D10 GPI-TCR α and β constructs (50 μ g of each plasmid) were electroporated into BW5147 cells, and cells were initially selected in methotrexate (MTX) at a concentration of 50 nM. After amplification to 500 μ M MTX, the amount of both TCRs on the cell surface was 5×10^6 molecules per cell for both 2C16 cells (2C GPI-TCR) and Ak19 cells (D10 GPI-TCR) as determined by Scatchard analysis.
32. Soluble TCRs were purified after cleavage from the cells by phosphatidyl inositol-phospholipase C (PI-PLC) by immunoadsorbent chromatography on columns of clonotypic mAbs 1B2 (28) for 2C and 3D3 for D10 (9) or with the C_{β} mAb H57-597 (29). Approximately 2×10^9 cells, grown either in Dulbecco's modified essential medium [supplemented with 500 μ M MTX, 10% heat-inactivated fetal calf serum, 2 mM l-glutamine, nonessential amino acids, and gentamicin (5 μ g/ml)] or in α -minimal essential medium (BioWhittaker, Gaithersburg, MD) supplemented with the same additives but with 1.3 μ M MTX, were harvested by centrifugation, washed once in phosphate-buffered saline (PBS), and resuspended in 12 ml of RPMI medium (BioWhittaker) containing 1 mM Hepes (pH 7.4), 1 μ M sodium pyruvate, and 2 units of PI-PLC (Sigma) for about 90 min at 37°C with frequent adjustment of the pH with 1 M NaHCO₃. The supernatant was clarified by centrifugation (3500 rpm for 10 min in the Sorvall HB1000 rotor) then passed through a 0.22- μ m filter and applied to immunoadsorbent columns prepared from protein-A-purified mAbs coupled to Affiprep 10 (Bio-Rad). After washing with PBS, bound TCR was eluted with either glycine HCl (0.1 M, pH 2.7) or potassium phosphate buffer (0.01 M, pH 11.5). Eluted protein was immediately neutralized, dialyzed against PBS, and concentrated by ultracentrifugation (Centricon 10) to >1 mg/ml.
33. Protein (either the purified 2C or D10 TCR) was diluted to a concentration of 100 μ g/ml in 10 mM sodium acetate at pH 4.6 and was coupled to the dextran-modified gold surface of a Sensor Chip CM5

- (Pharmacia) with standard coupling chemistry with *N*-hydroxysuccinimide and *N*-ethyl-*N'*-(3-dimethylaminopropyl)-carbodiimide hydrochloride in the Pharmacia BIAcore as described (12, 30). Purified MHC class I molecules sH-2L^d (consisting of the α 1 and α 2 domains of H-2L^d linked to the α 3 and COOH-terminus of Q10^b), sH-2K^b (α 1 and α 2 domains of H-2K^b linked to the α 3 domain of H-2D^d and the COOH-terminus of Q10^b), and sH-2D^d (α 1, α 2, and α 3 domains of H-2D^d and the COOH-terminus of Q10^b) were mixed with the indicated peptides at the indicated concentrations (Fig. 1), diluted into HBST [10 mM Hepes (pH 7.5), 150 mM NaCl, 3.4 mM EDTA, and 0.05% Tween-20], and injected over the 2C-coupled surfaces. Flow rates for the binding and dissociation phases were 5 μ l/min. Binary data files were transferred from the BIAcore to a Macintosh computer and analyzed and plotted with Igor (WaveMetrics, Lake Oswego, OR). All sensorgrams were normalized to a base line of 0 resonance units (RU). For the sensorgrams (Fig. 1, D and E), refractive index artifacts were corrected by subtraction of the sH-2D^d-p2CL background sensorgram.
34. A biosensor surface coupled with 2C TCR (Fig. 1) was exposed to complexes of sH-2L^d-p2CL at the indicated concentrations of p2CL or sH-2L^d. Equilibrium values (taken as resonance units at $t = 360$ s) of the concentration-dependent resonance units were fit to the four-parameter equation

$$y = \{[(a - d)/(1 + (x/c)^b)] + d$$

where a is the minimal RU; b is the slope factor; c is the value of x with half-maximal binding; and d is the maximal RU with the use of Kaleidagraph (Synergy Software, Reading, PA). For Fig. 2D, $a = 15.5 \pm 44.8$; $b = 1.2 \pm 0.15$; $c = 0.047 \pm 0.0053$; $d = 1857.2 \pm 73.4$; $\chi^2 = 6089.7$; and the correlation coefficient, R , is 0.99891. Values for the concentration of preparations of sH-2L^d are based on the protein concentration corrected for the proportion of molecules capable of binding peptide, which was estimated to be 40% in an assay of peptide-depen-

dent epitope induction (12, 16). For the competition curve (Fig. 2E), sH-2L^d (500 μ g/ml, saturated with p2CL) was mixed with graded amounts of the 2C TCR and injected over the biosensor surface coupled with the 2C TCR.

35. Data points for the experiment of Fig. 2C were fit for the 401 data points of the first 200 s for the association phase with use of the program Igor to the single exponential equation

$$B_t = B_{\infty} - B_{\max} \exp(-k_{\text{obs}} t)$$

where B_t was the amount bound in RU at time t , B_{∞} was the amount bound at equilibrium, and B_{\max} was the maximum bound (B_{\max} always was $\geq 0.9 B_{\infty}$). For fitting to a double exponential equation (descriptive of two simultaneous independent processes), we used the equation

$$B_t = B_{\infty} - [B_{\max, \text{fast}} \exp(-k_{\text{obs, fast}} t) - [B_{\max, \text{slow}} \exp(-k_{\text{obs, slow}} t)]$$

where fast and slow components were considered. The dissociation phase was fit to the single exponential expression

$$B_t = B_0 \exp(-k_{\text{off}} t)$$

or to the double exponential expression

$$B_t = B_{\text{fast}} \exp(-k_{\text{off, fast}} t) + B_{\text{slow}} \exp(-k_{\text{off, slow}} t)$$

Residuals, the differences between the fit curve and the experimental data, are plotted. The larger residuals were characteristic of the curves with higher concentrations of sH-2L^d.

36. Y. Sykulev *et al.*, *Immunity* 1, 15 (1994).
37. We thank our colleagues J. Berzofsky, S. Kozlowski, A. Minton, S. Sadegh-Nasseri, E. Shevach, M. Sitkovsky, E. A. Padlan, and K. Parker for their advice and comments on the manuscript; S.-C. Hong and C. Janeway for the D10 cDNA and 3D3 clonotypic mAb; J. Coligan for peptides; and C. Hoes for his help. A.L.M.B. was supported by a grant from NIH.

1 April 1994; accepted 21 June 1994

Activation of a Cerebellar Output Nucleus During Cognitive Processing

S.-G. Kim, K. Uğurbil, P. L. Strick*

Magnetic resonance imaging was used to examine the involvement of the dentate nucleus of the cerebellum in cognitive operations. All seven people examined displayed a large bilateral activation in the dentate during their attempts to solve a pegboard puzzle. The area activated was three to four times greater than that activated during simple movements of the pegs. These results provide support for the concept that the computational power of the cerebellum is applied not only to the control of movement but also to cognitive functions.

The cerebellum is a part of the central nervous system and is essential for the proper control of limb and eye movements (1, 2). This brain structure consists of a large cortex, which processes input, and several deep nuclei, which process output. The lateral cerebellar cortex and the lateral deep nucleus, the dentate, underwent a marked

expansion in the course of hominid evolution (3).

Evidence for the involvement of the cerebellum in aspects of motor learning and in the adaptive modification of motor output is accumulating (2, 4). On the other hand, there has been controversy about the participation of the cerebellum in nonmotor, cognitive operations (5-7). Leiner *et al.* (5, 6) have argued that the increase in the size of the dentate nucleus is paralleled by an increase in the size of the cortical areas influenced by cerebellar output and, consequently, by an expansion of cerebellar function to include involvement in some language and cogni-

tive tasks. Perhaps some of the best support for this view comes from the results of a positron emission tomography (PET) study that showed activation in an inferior and lateral part of the cerebellum during a rule-based word generation task (8, 9). This activation was spatially separate from that found during motor tasks, including speech. Other imaging studies have reported activation in the inferior lateral cerebellum during silent counting and mental imagery (10).

The activation of the cerebellum observed in earlier studies reflects changes occurring largely, if not exclusively, in the cerebellar cortex. Large modulations in the input to the cerebellar cortex can take place without leading to observable changes in motor behavior (11). Thus, evidence that cerebellar output from the deep nuclei participates in cognitive processing has been lacking. To examine this issue, we used magnetic resonance imaging (MRI) to study functional activation of the dentate nucleus during a task that included a cognitive component. The greater spatial resolution of MRI (12) relative to other imaging methods allowed us to visualize activity changes in the dentate.

Seven healthy human volunteers participated in these experiments (13). Par-

S.-G. Kim and K. Uğurbil, Center for Magnetic Resonance Research, Department of Radiology, University of Minnesota Medical School, Minneapolis, MN 55455, USA.

P. L. Strick, Research Service (151), Veterans Administration Medical Center, and Departments of Neurosurgery and Physiology, State University of New York Health Science Center, Syracuse, NY 13210, USA.

*To whom correspondence should be addressed.